

# A PROCEDURE FOR THE ESTIMATION OF THE SHAPE IMPERFECTIONS OF A COMPOSITE PANEL IN ORDER TO REPRODUCE ITS POSTBUCKLING EVOLUTION

Antonio Blázquez<sup>1</sup>, Jesús Justo<sup>2</sup>, José Reinoso<sup>3</sup> and Federico París<sup>4</sup>

Grupo de Elasticidad y Resistencia de Materiales, Escuela Técnica Superior de Ingeniería,  
Universidad de Sevilla, Camino de los Descubrimientos s/n, 41092 Sevilla, Spain

Email: <sup>1</sup>abg@us.es, <sup>2</sup>jjusto@us.es, <sup>3</sup>jreinoso@us.es, <sup>4</sup>fparis@us.es

Web Page: <http://www.germus.es>

**Keywords:** buckling, postbuckling, geometric imperfections

## Abstract

In the analysis of buckling and postbuckling of plates and shells, large discrepancies between the experimental measures (which frequently present lot of dispersion) and the analytical or numerical predictions usually appear. Imperfections inherent to the test (geometry, boundary conditions, material, etc) have been accepted as the explanation for this fact. Obviously, two panels are never identical, even if they are made with the same manufacturing process. Thus, it is really difficult to justify a design procedure that takes advantage of the postbuckling residual strength. Currently, modern numerical techniques can simulate the behaviour of real structures, but results depend very much on the inputs: boundary conditions and loads, material properties, geometric imperfections, residual stresses, etc. If imperfections are unknowns, predictions of buckling loads and postbuckling behaviour cannot be improved. In this paper two procedures to estimate imperfections from experimental measurements performed during the pre-buckling evolution of the panel, are proposed. These procedures have been checked using a Montecarlo simulation process with numerical solutions.

## 1. Introduction

In the analysis of buckling and postbuckling of plates and shells, large discrepancies between the experimental measurements, which frequently present a lot of dispersion, and the analytical or numerical predictions appear. The imperfections inherent to the test have been accepted as the explanation for this fact. This was already highlighted in pioneering works, see [1] (where word *imperfection* appears more than 500 times) for classic references.

Obviously, two panels are never identical, even if they are made with the same manufacturing process, because imperfections of each one will be always different. Thus, it is really difficult to justify a design procedure that, based exclusively on the analytical or numerical analysis of the panels, takes advantage of the postbuckling reserve of strength; a sufficient and really high number of experiments are needed to decide the 'knock-down' factor (following the current design philosophy) that has to be used in order to ensure the safety and functionality of a shell structure. In fact, an International Imperfection Data Bank has been established for this task [2].

Most of the experiments in the literature used many strain gages, usually bonded in pairs back-to-back and some linear variable differential transformers (LVDT) [3, 4], Moiré interferometry [5] or other optical techniques [6] for describing the results and identifying the buckling and postbuckling patterns.

Currently, modern numerical techniques can simulate the behaviour of real structures but results depend very much on the inputs [2, 5, 7]: the boundary conditions and loads, the material properties (which increased interest for composites), the geometric imperfections (thickness distribution and shape), residual stresses, etc. If imperfections are unknown, predictions of buckling loads and postbuckling behaviour cannot be improved, *no matter how sophisticated our codes are and how large and fast our computers become* [2]. Sometimes, inputs can be improved from nondestructive techniques, a close interaction between numerical analysis and experimental tests being necessary. These are the cases of vibration correlation techniques for fixing boundary conditions, scan of the surface for geometric imperfections, X-ray techniques for residual stresses, etc.

It is generally accepted that the most critical imperfections are those associated to the geometric shape and boundary conditions. Focusing our attention on the geometric imperfections, usually, a grid is defined on the panel and LVDT, [3, 4], or other noncontacting probes (for example laser displacement sensors, preventing the 'small' distortion introduced by the own probes), [8], on a trolley car or similar, are used to survey the surface of the panel. A revision of the evolution of measure techniques for shell imperfections (specifically geometric and boundary conditions imperfections) is presented in [2]. With the right device, the actual position of each node of the numerical model can be determined, but this is a really hard work (specifically for stiffened panels) because the grid for the measurements should coincide with the finite element mesh. Thus, a linear combination of independent functions (for example Fourier series or buckling modes) is assumed and a best-fit procedure is used to approximate the actual shape. This way has proved to be an excellent tool for obtaining accurate results with only a few functions in lab specimens [3, 4, 7, 8, 9]. Nevertheless, the extension to full scale structures is not easy, and could continue to be the reason why practical engineers are reluctant to accept and assimilate the findings of theoreticians [9].

In this paper, taking into account that imperfection effects can be also detected during the pre-buckling phase, a systematic procedure for determining the set of coefficients of a linear combination of assumed functions to approximate the actual geometry of the panel are developed. Obviously, the effects of imperfections in pre-buckling stages will be larger or smaller depending on the sensitivity of the particular measure to the actual configuration of the panel. For example, back-to-back strain gages are more sensitive than a measurement of the shortening, and it is preferable to place the gages at positions with symmetric deformation (maximum curvature) than at other with antisymmetric deformation (zero curvature). Here procedures are only applied to the estimation of geometric shape imperfections, but none difficulties are glimpsed to extend them to other sources of imperfections.

## 2. Problem statement

Let us consider a general problem of which  $N$  experimental measurements,  $\varepsilon_b$  ( $b = 1, \dots, N$ ), are available. These measurements will depend on the loads, boundary conditions, material properties, geometry, etc:

$$\varepsilon_b = E_b(\text{loads, boundary conditions, material, geometry, ...}). \quad (1)$$

As usual, the real geometry of the panel will be approximated adding to the ideal configuration a linear combination of  $K$  adimensional functions,  $u_i^k(\mathbf{P})$  ( $k = 1, \dots, K$ ), which represent the assumed distribution of imperfections (using Einstein summation convention):

$$x_i(\mathbf{P}) \approx x_i^0(\mathbf{P}) + \sum_{k=1}^K c_k u_i^k(\mathbf{P}) = x_i^0(\mathbf{P}) + c_k u_i^k(\mathbf{P}) \quad \rightarrow \quad \mathbf{x}_i = \mathbf{x}_i^0 + (\mathbf{c})^T \mathbf{u}_i, \quad (2)$$

$x_i(\mathbf{P})$  ( $i = 1, 2, 3$ ) being the actual position of the point  $\mathbf{P}$  of the panel,  $x_i^0(\mathbf{P})$  the position of that point in the ideal configuration,  $u_i^k(\mathbf{P})$  ( $k = 1, \dots, K$ ) the function serie used to approximate the actual shape of the

panel, and  $c_k$  ( $k = 1, \dots, K$ ) the coefficients wanted to be estimated;  $\mathbf{x}_i$ ,  $\mathbf{x}_i^0$ ,  $\mathbf{u}_i$  and  $\mathbf{c}$  are the corresponding vectors.

Without loss of generality, buckling modes of the ideal panel (first  $K$  modes) are used as approximation functions in this paper. Assuming all variables were correctly evaluated except the shape of the geometry, each measurement can be expressed as:

$$\varepsilon_b \approx E_b(x_i^0 + c_k u_i^k) = E_b(x_i^0, c_k, u_i^k). \quad (3)$$

Experimental measurements are grouped in the vector:  $\boldsymbol{\varepsilon} = (\varepsilon_1, \varepsilon_2, \dots, \varepsilon_N)^T$ , the goal being to find the relation:

$$\mathbf{c} = \mathbf{F}(\boldsymbol{\varepsilon}), \quad (4)$$

$\mathbf{F}$  being a vectorial function. This type of problems are called *supervised learning*, experimental measurements are denoted as *inputs*, *predictors* or *independent variables*; and coefficient defining the imperfection shape distribution are denoted *outputs*, *responses* or *dependent variables* [10].

Generally, the problem can not be solved with traditional method because  $N \neq K$ ; in fact it should be  $N \geq K$  to avoid multiple solutions, and what is more  $N \gg K$  being an usual choice in order to avoid 'over-fitting'. The most simple procedures to solve this type of problems are linear models based on nearest neighbors and least squares methods.

### 3. Nearest neighbors method (NNM)

This method is appropriate for a classification problem. In this way, (4) can be posed as the problem of a traveler trying to go from a departure station, which is identified as the ideal geometry ( $x_i^0 = 0$ ), to the nearest station to a certain position, which is defined as the actual geometry of the panel ( $x_i$ ), following specific routes.

Each station,  $s$ , is defined by a vector of perturbation coefficient,  $\mathbf{c}^s = c_k^s$  ( $k = 1, \dots, K$ ), which define the geometry:

$$\mathbf{x}^s = \mathbf{x}^0 + (\mathbf{c}^s)^T \mathbf{u}. \quad (5)$$

The numerical estimations of the strain gage measurements at this new station:  $\boldsymbol{\varepsilon}^s = \varepsilon_b^s$  ( $b = 1, \dots, N$ ), are obtained solving, for example, the corresponding finite element simulation. The distance to the target is defined as the modulus of the vector from the experimental data,  $\boldsymbol{\varepsilon}$ , to these numerical results,  $\boldsymbol{\varepsilon}^s$ :

$$d^s = |\boldsymbol{\varepsilon}^s - \boldsymbol{\varepsilon}|. \quad (6)$$

One station is nearer than another if the distance for the first one is lower than that for the second one.

To go from a station to another, routes have to be defined. Here, variation of each perturbation coefficients in positive and negative directions are used. Thus if  $K$  modes are used,  $2K$  routes are defined from each station, each one being defined by  $\Delta \mathbf{c}_m = (-1)^m \zeta_{mi}$ ,  $m = 1, \dots, 2K$  and  $\zeta_{mi} = \zeta$  if  $m = 2i$  or  $m = 2i - 1$  and  $\zeta_{mi} = 0$  otherwise;  $\zeta$  being a number that define the length of the journey.

For each route numerical estimation of strain measurements are computed and the distance calculated. From all the end of routes, that reaching to the target nearest position is selected as the new departure station, and the process re-start. If all the stations were farther from the target than the departure station of the step, the length of the journey is reduced (for example to the half) and the algorithm repeated until the length of the journey was smaller than a reference. A flowchart of the proposed algorithm is shown in Fig. 1a.

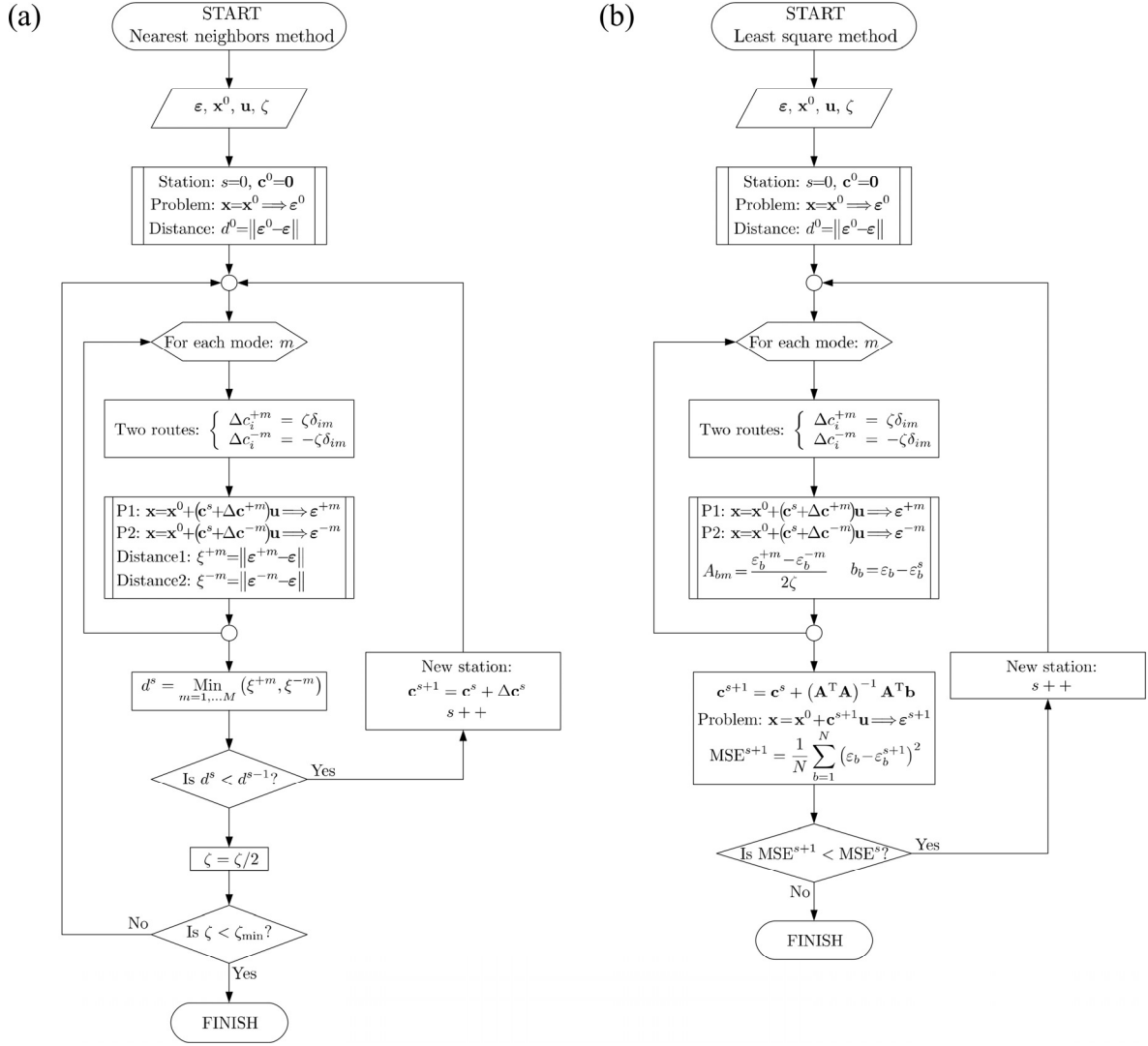


Figure 1. Flowcharts: (a) nearest neighbors method, and (b) least square method.

#### 4. Least square method (LSM)

Assuming that imperfections are small and that Eq. (3) admits a Taylor serie expansion in  $c_k$  ( $k = 1, \dots, K$ ), coefficients about the ideal configuration,  $c_k^0 = 0$ :

$$\varepsilon_b \approx \varepsilon_b^0 + \frac{\partial \mathbf{E}_b}{\partial c_k} c_k. \quad (7)$$

$\varepsilon_b^0$  ( $b = 1, \dots, N$ ) being the results of the ideal configuration for the measurement  $b$ , which are obtained from either a numerical or an analytical model, as can not be obtained otherwise.

Derivatives in Eq. (7) can be approximated using the forward, backward or central finite differences. However, the last one yields a more accurate approximation, in which case:

$$\frac{\partial \mathbf{E}_b}{\partial c_k} = \frac{\mathbf{E}_b(x_i^0, c_j = \zeta \delta_{kj}, u_i^k) - \mathbf{E}_b(x_i^0, c_j = -\zeta \delta_{kj}, u_i^k)}{2 \zeta}, \quad (8)$$

$\zeta$  being a sufficiently small number (which in fact corresponds to the length of the journey) and  $\delta_{kj}$  a Kronecker delta. Using this approximation in Eq. (7):

$$\varepsilon_b \approx \varepsilon_b^0 + \frac{E_b^{+k} - E_b^{-k}}{2 \zeta} c_k. \quad (9)$$

where  $E_b^{+k} = E_b(x_i^0, c_j = \zeta \delta_{kj}, u_i^k)$  and  $E_b^{-k} = E_b(x_i^0, c_j = -\zeta \delta_{kj}, u_i^k)$ . These values are calculated from the corresponding analytical or numerical model.

Applying Eq. (9) for each experimental measurement, the following system of equation is obtained:

$$\varepsilon_b - \varepsilon_b^0 = \frac{E_b^{+k} - E_b^{-k}}{2 \zeta} c_k \quad \rightarrow \quad \mathbf{b} = \mathbf{A} \mathbf{c}. \quad (10)$$

This system has  $N$  equations and  $K$  unknowns and it is solved posing the problem as one of minimizing an objective function, the most usual being the *mean square error* (MSE). In this case, the final system results:

$$\mathbf{A}^T \mathbf{b} = \mathbf{A}^T \mathbf{A} \mathbf{c} \quad \rightarrow \quad \mathbf{c} = (\mathbf{A}^T \mathbf{A})^{-1} \mathbf{A}^T \mathbf{b}. \quad (11)$$

It is a trip (following a parallelism with the NNM) of a single leg, the route being computed by minimizing the MSE.

Using up this idea, the process can be easily enhanced performing another step where the departure station/geometry is defined by the arrival station of the previous step. In this case, referring  $s$  to the new estimated geometry, equations are modified as follows:

$$\varepsilon_b = \varepsilon_b^{s-1} + \frac{E_b^{+k} - E_b^{-k}}{2 \zeta} (c_k^s - c_k^{s-1}) \quad \rightarrow \quad \varepsilon_b - \varepsilon_b^{s-1} = \frac{E_b^{+k} - E_b^{-k}}{2 \zeta} \Delta c_k^s$$

$$\Delta \mathbf{c} = (\mathbf{A}^T \mathbf{A})^{-1} \mathbf{A}^T \mathbf{b} \quad (12)$$

where  $\Delta c_k^s = c_k^s - c_k^{s-1}$ ,  $c_k^s$  being the coefficients for the new enhanced estimation of the geometry and  $c_k^{s-1}$  the coefficients of the estimation of the previous step. Now,  $E_b^{+k} = E_b(x_i^0, c_j = c_j^{s-1} + \zeta \delta_{kj}, u_i^k)$  and  $E_b^{-k} = E_b(x_i^0, c_j = c_j^{s-1} - \zeta \delta_{kj}, u_i^k)$ .

The procedure will continue until an specified end-condition was satisfied. Notice that we can not consider a bound of the minimum square error (MSE) as end-condition because there is not guarantee that it can be fulfilled. An obvious condition is that the MSE between two consecutive steps increases.

Nevertheless, we have considered a modification of this condition telling, on the one hand, the difference between the route (i.e. the orientation of the pseudo-vector  $\Delta \mathbf{c}$ ), and on the other hand the length (i.e. the modulus of  $\Delta \mathbf{c}$ ). First we assume that LSM determines both: route and length, but if MSE does not decrease in the step, the route (orientation) is maintained but the length is divided by 2. Process is repeated until the length of the trip was smaller than a minimum. A flowchart of the proposed algorithm is shown in Fig. 1b.

## 5. Benchmark problem

In this section we consider the problem shown in Fig. 2. It is a square plate simply supported on its four edges and compressed in the  $y$ -direction. Material is a carbon fiber composite whose properties are shown in Fig. 2, subindex 1 referring the fibre direction. Four 12-ply stacking sequences were analysed:  $[0]_{12}$ ,  $[90]_{12}$ ,  $[45]_{12}$  and  $[45, -45, 0, 90, 45, -45]_8$ ; 0 being the direction of the load ( $y$ -direction) and ply width being 0.13 mm.

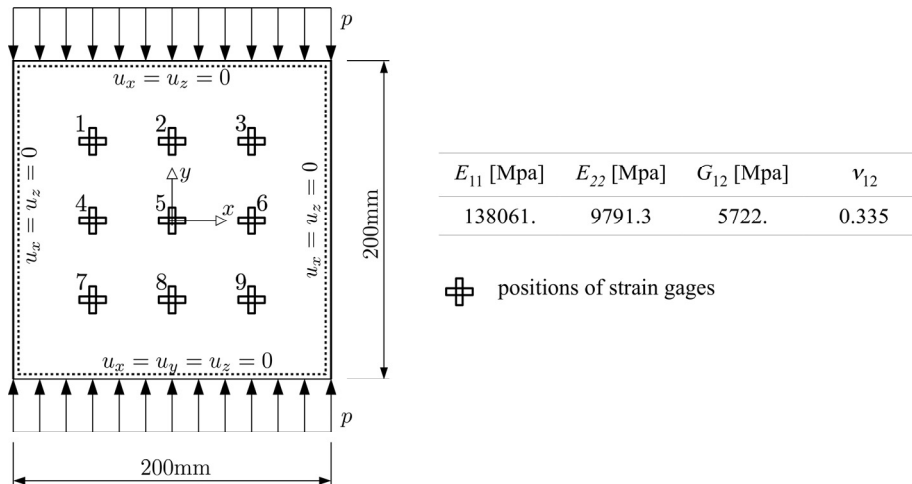


**Figure 2.** Benchmark problem: geometry, load and boundary conditions and material.

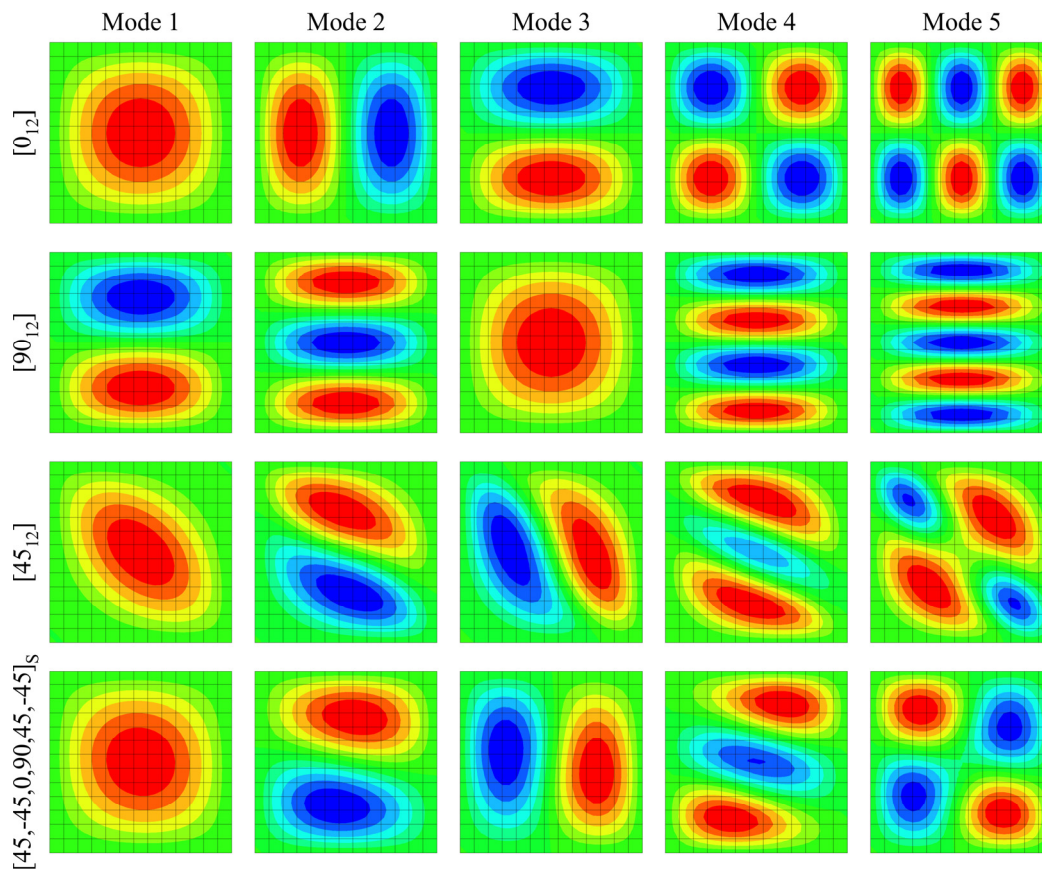


**Figure 3.** Benchmark problem: first five buckling modes of the configurations.

To estimate the confidence on the procedures, the first step must be to work on a perfectly known panel to verify if the correct values of the coefficients can be obtained. This evaluation was carried out virtually considering the buckling modes shown in Fig. 3. If this step leads to satisfactory results, the next step would be the manufacturing of a specific panel. As this is an expensive procedure involving sophisticated measuring techniques and many tests, it is necessary to get a robust estimation of the capacities of the proposed procedures.

First, a combination of the coefficients  $c_1$  to  $c_5$  was randomly obtained, assuming  $-2 \text{ mm} \leq c_i \leq 2 \text{ mm}$  ( $i = 1, \dots, 5$ ), for the definition of our virtual specimen. This specimen was solved numerically using a  $13 \times 13$  mesh of conventional parabolic shell elements with reduced integration (S8R Abaqus® element), and strains at the locations shown in Fig. 2 were extracted (36 data: 18 front and 18 back,  $x$  and  $y$  directions); these results were the ‘measurements’ of the virtual test. Then NNM or LSM was applied and the coefficients obtained were compared with the real ones.

One hundred virtual tests were performed for NNM and another 100 for LSM, using the same 5 modes (see Fig. 3) and mesh. Two end-conditions were considered with respect to the distance,  $d$ , Eq. (6): (i)  $d \leq 0.01$ , or (ii)  $d$  increases for the new step. The rate of success (i.e. the number of tests for which the exact values were reached) give us the confidence of the procedure. Although virtual tests were different for both methods, the number of them is large enough to draw statistical conclusions.

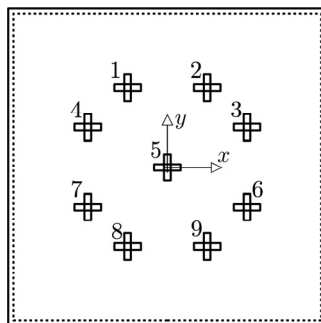
A summary of the results is shown in Table 1. The  $N_{st}$  columns refer to the average number of stations visited, the  $\text{Max}(N_{st})$  columns show the maximum number of stations visited for all the tests, and the  $T_{ex}$  columns mean the number of tests which MSE is lower than 0.0001 (the square of the end condition), in which case, the obtained final configuration being considered correct.

**Table 1.** Benchmark problem: summary of the results.

Configuration	Nearest neighbors method			Least square method		
	$N_{st}$	$\text{Max}(N_{st})$	$T_{ex}$	$N_{st}$	$\text{Max}(N_{st})$	$T_{ex}$
$[0_{12}]$	40.0	198	77	11.6	31	61
$[90_{12}]$	62.3	185	43	11.7	40	68
$[45_{12}]$	30.8	134	94	8.0	10	100
$[45, -45, 0, 90, 45, -45]_s$	34.0	94	95	7.6	14	100

From the data shown in this table, LSM seems to be the most recommended procedure because it is much faster and more robust.

It is also noticeable the fact that, for both methods, the success ratio is near 1 for  $[45_{12}]$  and  $[45, -45, 0, 90, 45, -45]_s$  laminates, whereas it is only about 2/3 for  $[0_{12}]$  and  $[90_{12}]$ . We attribute this difference to the fact that strain gages located at positions 2, 4, 5, 6 and 8 (20 from 36 gages), see Fig. 2, are not very sensitive to the effect of some modes because they are located at an antisymmetric line (for example: gages 2, 5 and 8 for mode 1 of  $[0_{12}]$  configuration; or gages 2, 4, 5, 6 and 8 for mode 4 of  $[90_{12}]$  configuration). On the contrary, this does not occur for the other two configurations. To checks this, gages were re-located at the position shown in Fig. 4 and the aleatory tests repeated for these two configuration (now only using the LSM). The result summary is shown in the same figure, success ratios increasing till 0.95 for both configurations.



Configuration	$N_{st}$	$\text{Max}(N_{st})$	$T_{ex}$
$[0_{12}]$	10.7	31	95
$[90_{12}]$	10.8	32	96

**Figure 4.** Benchmark problem: alternative position of the strain gages.

## 6. Conclusions

A general procedure for the estimation of initial geometric imperfections has been presented. It takes advantage from the fact that, although small, imperfection effects can be detected also at the pre-buckling stage. Thus, comparing the actual evolution with numerical solutions of the problem, the coefficients of the function serie used for the adjustment of the geometry can be obtained.

Two algorithms have been analysed and compared using a Montecarlo process with 100 virtual tests. Both of them progress approaching the experimental measurements step-by-step. The first one tries some previously considered combinations (routes and distance) of the coefficient increments, and that combination which provides the nearest to the experimental measurement results is selected. The second one obtains the combination of the coefficients using a least square method. In any of them, the new combination is the departure station for a new step. Process ends when no rapprochement is obtained.

The approach based on the least square method has proved to be faster and stronger than the nearest neighbors method. Next step in this research is the application of this technique to an actual panel. In this sense, some plates will be manufactured and tested.

## Acknowledgments

This research was conducted with the support of the Spanish Ministry of Economy and Competitiveness (Project MAT2015-71036-P). This funding is gratefully acknowledge.

## References

- [1] N.F. Knight Jr., and M.P. Nemeth. *Stability analysis of plates and shells. A collection of papers in honor of Dr. Manuel Stein*. NASA/CP-1998-206280 (1998).
- [2] J. Singer and H. Abramovich. The Development of Shell Imperfection Measurement Techniques. *Thin-Walled Structures*, 23: 379-398, 1995.
- [3] H. Abramovich, T. Weller and C. Bisagni. Buckling behavior of composite laminated stiffened panels under combined shear-axial compression. *Journal Aircraft*, 45: 402-413, 2008.
- [4] Blázquez A, Reinoso J, París F and Cañas J. Postbuckling behavior of a pressurized stiffened composite panel – Part II: Numerical analysis. Effect of the geometrical imperfections. *Composite Structures*, 94: 1544-1554, 2012.
- [5] M.W. Hilburger and J.H. Starnes Jr. Effects of imperfections on the buckling response of compression-loaded composite shells. *International Journal of Nonlinear Mechanics*, 37: 623-643, 2002.
- [6] A. Blázquez, J. Justo, R. Roig and F. París. Experimental postbuckling study of pre-conformed composite plates. *Proceedings of the 20th International Conference on Composite Materials ICCM-20. Copenhagen, Denmark*, July 19-24 2015.
- [7] J.W. Hutchinson. Shell Buckling - the old and the new. *New England Workshop on the Mechanics of Materials and Structures*, Link: <https://www.youtube.com/watch?v=8iIPEojHB1g>, October 14th, 2017.
- [8] C. Bisagni. Numerical analysis and experimental correlation of composite shell buckling and post-buckling. *Composite Part B: Engineering*, 31: 655-667, 2000.
- [9] J. Arbocz and C.D. Babcock Jr. Prediction of buckling loads based on experimentally measured initial imperfections. In: *Buckling of structures*. Budiansky B (ed.), 1976.
- [10] T. Hastie, R. Tibshirani and J. Friedman. *The elements of statistical learning. Data mining, inference, and prediction*. Springer Series in Statistics, Springer, ISBN 978-0-387-84857-0, 2016.